Journal of Theoretical and Applied Physics (JTAP), Special Issue: AICIS'23-Article 09

Proceeding of the 3rd Annual International Conference on Information and Sciences 2023, University of Fallujah, Iraq

https://dx.doi.org/10.57647/j.jtap.2024.si-AICIS23.09

Gold-capped Fe_3O_4 nanoparticles with a magnetic field by damaging their DNA and generating more oxygen radicals, colon cancer cells can be made to die

Waleed K. Abdulkadhim[1,*], Ayad B. Sahi[2], Mahdi A. Mohammed[3]

[1]*Department of Pathological Analyzes, College of Science, Wasit University, Al Kut, Iraq.*
[2]*Hospital Fairooz, Wasit, Iraq.*
[3]*Department of Physics, College of Science, Wasit University, Al Kut, Iraq.*

[*]**Corresponding author:** waleed.k@uowasit.edu.iq

Original Research

Published online:
15 June 2024

Abstract:

Using a hydrothermal technique, the gold (Au)-capped magnetite nanoparticles (Fe_3O_4) in the current work were created. TEM, SEM and FTIR were used to analyze the characteristics of the Fe_3O_4-Au MNPs and confirm the accuracy of the synthesized Fe_3O_4-Au. The size range of (5 – 15) nm was observed for Fe_3O_4–Au. By using the MTT assay, the impact of Fe_3O_4-Au on the proliferation of colon cancer (HT-29) cells was evaluated. Additionally, the cytotoxicity effects of Fe_3O_4-Au on (HT-29) cells were evaluated in both the absence and presence of alternating magnetic field (AMF) and laser photothermal therapy. According to the findings, Fe_3O_4-Au caused (HT-29) cells' proliferation to be inhibited, which led to their planned demise. Cytotoxic activity against (HT-29) cells increased when exposed to NIR laser irradiation, however greatly elevated cytotoxic activity was seen after being exposed to induction heating with AMF. With regard to photothermal therapy for cancer cells, the current studies indicate that Fe_3O_4-Au with NIR laser and AMF may be promising.

Keywords: Fe_3O_4-Au MNPs; (HT-29) cells'; Hydrothermal technique; Photothermal therapy

1. Introduction

A significant issue for human society has always been cancer. Cancer continues to be one of the major causes of mortality worldwide, despite extensive research and progress over the past ten years. Recent data [1–3] indicate that cancer is the second leading cause of mortality worldwide, trailing only cardiovascular disease. Radiation, chemotherapy, and surgery are currently used as cancer treatments. These techniques, however, aren't just employed to treat cancer. Numerous studies have found that the results of two or three therapies combined are better and more successful than those of a single therapy. Nevertheless, healthy cells typically die as well, and the patient could have adverse effects. Researching innovative therapies is crucial for the management of cancer because of this [4, 5]. The use of nanotechnology in cancer treatment has grown significantly in recent years. Enhanced tumor cell killing, protection against radiation side effects, and increased treatment sensitivity are some of its advantages in medication development. In the interim, there has been a great deal of interest in the application of metal oxide nanoparticles in the treatment of cancer. Natural metal oxides can be produced inexpensively and are rather prevalent in nature. As a result, research in this field is concentrated on creating affordable pharmaceutical goods, and the production of these nanoparticles may be one of the easiest methods [6, 7]. Due to their biocompatibility, physicality, low toxicity, durability, ability to stop the cell cycle, and magnetic properties, One of the most significant metal nanoparticles is magnetic iron oxide [8, 9]. The ability of magnetic iron oxide nanoparticles to kill cancer cells has also been established [10, 11]. Many malignancies, including blood, lung, pancreatic, and prostate cancer cells, have been treated with magnetic iron oxide nanoparticles found in chemotherapeutic substances [12]. Previous studies have shown that oxidative stress and

the generation of oxygen-free radicals caused by magnetic nanoparticles might cause cells to undergo apoptosis [13–15]. The mechanism by which nanomaterials operate on different body locations is still unknown, despite substantial research on the impacts of nanomaterials on mitochondrial damage, oxidative stress, genomic damage, altered cell cycle settings, and denaturation of proteins [16, 17]. Reactive oxygen species (ROS) production and subsequent oxidative stress are two potential mechanisms for nanoparticles. ROS and oxidative stress alter calcium levels in cells, trigger inflammatory cell responses, activate transcription factors (p53 is one of these transcription factors), and increase the production of cytokines, which ultimately results in apoptosis [18, 19]. Nanomaterials also significantly contribute to oxidative stress, lipid peroxidation, DNA degradation, membrane deterioration, and ultimately cell death [20]. Thus, by lowering side effects, they can produce treatments that are efficient and eradicate the tumor [21]. Our understanding of how Superparamagnetic Iron Oxide Nanoparticles trigger Apoptosis in HT-29 cells will be improved as a result of this study's utilization of this information. Because of their distinctive magnetic features, extremely low toxicity, high biocompatibility, outstanding biodegradability, and reactive surface that is easily modified with biocompatible coatings like gold (Au) metal, targeted drug and gene delivery systems are particularly advantageous. Fe_3O_4 NPs are chosen over other magnetic materials due to the presence of the Fe^{2+} state, which may function as an electron donor.

2. Materials and methods

2.1 Chemicals

From Beijing Chemicals in China, the following substances were purchased: (EG) glycol, (NaOAc) anhydrous sodium acetate, sodium citrate, ethanol, ETA, $HAuCl_4$, and ferric chloride hexahydrate ($FeCl_3$•$6H_2O$). Sigma-Aldrich in Shanghai, China, provided Calcine AM for purchase, all the materials have pure 99%.

2.2 Preparation of Fe_3O_4-Au NPs

By employing Fe_3O_4 particles as the starting point for the reduction of Au^{3+}, Fe_3O_4-Au NPs were created using a hydrothermal technique. continually stirring, prepared and heated at 90 °C was 100 mL of sodium citrate (2.29 g/mL). Then, immediately, 40 mg of Fe_3O_4 NPs were added to the mixture. After being heated for 15 minutes, 5 mL of the $HAuCl_4$ solution (0.01 mol/L) was added. It was then cooled to room temperature while being vigorously stirred for 15 - 20 minutes. The resulting colloidal solution was separated by using a magnetic field. After rinsing and suspending the magnetically separated Fe_3O_4-Au NPs in 20 mL of doubly deionized water, they were then dried. The nanoparticles were subsequently put through a series of alternate washing cycles using either deionized water or ethanol, and they were then allowed to dry in a vacuum (overnight at 60 °C).

2.3 Characterization of Fe_3O_4-Au MNPs

TEM (Philips) and scanning electron microscopy (TESCAN, Vega III, Czech Republic) were used to analyze the size and morphological properties of the MNPs. One drop of the MNPs solution was applied to a (Cu grid) that was covered in gold and had a mesh size of approximately 200 to prepare the sample for TEM analysis. 8000 Series Shimadzu Fourier transform infrared spectroscopy (FTIR) apparatus was used to examine the molecular vibrations in produced samples.

2.4 Maintaining cell cultures

10% fetal bovine serum, 100 units/mL penicillin, and 100 g/mL streptomycin were added to RPMI-1640 to support HT-29 cells. The cells were passaged with trypsin-EDTA, reseeded at 80% confluence twice weekly, and incubated at 37 °C [22].

2.5 Cytotoxicity assays

To examine the cytotoxic effects of X-SUBSTANCES, 96-well plates were employed for the MTT test [23]. We seeded the cell lines with 104 cells per well. After 24 hours or after the formation of a confluent monolayer, cells were exposed to X-SUBSTANCES at varied concentrations in both the presence and absence of a magnetic field and a laser. By removing the medium, and adding 28 L of an MTT solution with 2 mg/mL, 72 hours after treatment, cell viability was assessed by treating the cells for 2.5 hours at 37 °C. After the MTT solution was withdrawn from the wells, the remaining crystals were solubilized by adding 130 L of DMSO (dimethyl sulfoxide), and they were then incubated at 37 °C for 15 min while being shaken. The experiment was done in triplicate, and the absorbency at 492 nm was measured using a microplate reader. The rate at which cell growth was inhibited, or the percentage of cytotoxicity, was determined using the equation shown below:

$$\text{Inhibition rate} = \frac{A - B}{A * 100} \quad (1)$$

where the optical density of the control is denoted by A, and that of the samples is denoted by B.

To examine the morphology of the cells using an inverted microscope, the cells were seeded at a density of 1105 cells/mL into 24-well micro-titration plates and incubated for 24 h at 37 °C. Then, for 24 hours, cells were exposed to X-substances while also being exposed to a magnetic field and laser light. After the exposure period, the plates were dyed with a crystal violet stain and kept at 37 °C for an additional 10 - 15 minutes. Once all traces of the color were gone, the stain was gently washed with tap water. A digital camera mounted on the inverted microscope was used to take photographs as the cells were being seen at 100x magnification [24].

2.6 Statistical analysis

An unpaired t-test was utilized to statistically evaluate the gathered data using GraphPad Prism 9. The average SD of three separate measurements was used to display the results [25].

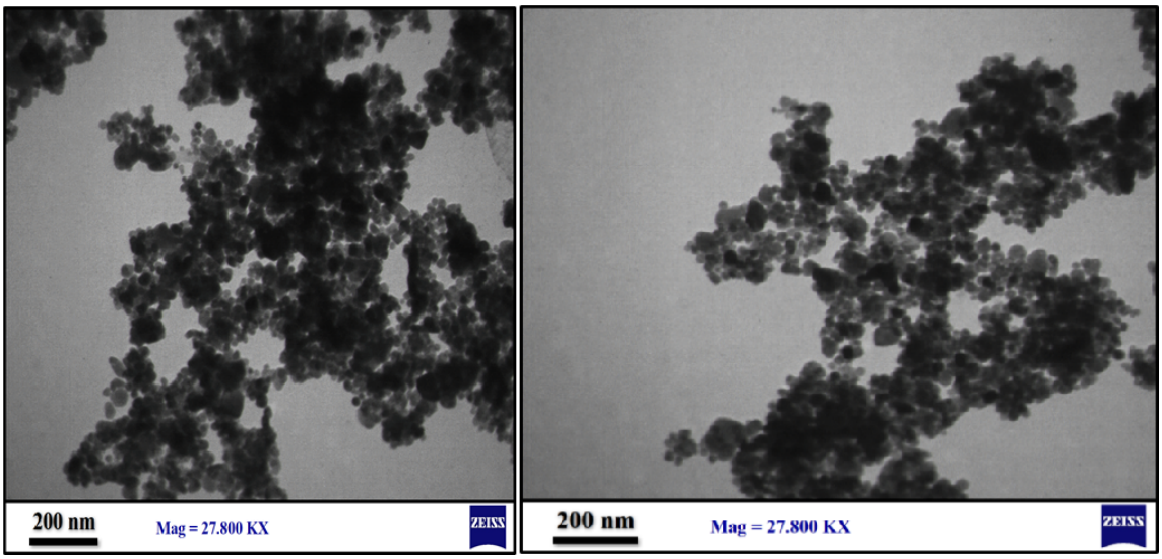

Figure 1. TEM images of Fe_3O_4-Au magnetic nanoparticles.

3. Results and discussion

3.1 Fe_3O_4-Au morphological characteristics

3.1.1 Transmission electron microscopy (TEM)

Using the TEM test, the morphological and size characteristics of Fe_3O_4-Au were investigated, see Fig. 1. The particles were roughly 5 – 12 nm in size and spherical in form. They were seen to have a well-dispersed state in relation to the Fe_3O_4-Au nanoparticles. It may therefore be inferred that covering the nanoparticles with Au caused a decrease in the size and agglomeration of the Fe_3O_4 nanoparticles while increasing their dispersion [26, 27].

3.1.2 Scanning electron microscopy

In order to further examine the shape and size of the created NPs, scanning electron microscopy was used. A scanning microscopy image of the same batch of samples, with a mean size of about 8 – 17 nm for Fe_3O_4–Au, is shown in Fig. 2. This graph demonstrates the high production of uniform NPs (Fe_3O_4-Au). These results suggested a potential selective absorption of the Au surfactant onto the beneficial properties of the particles, as the generated NPs were well within the required size for the effective delivery of the drugs included. potentially inhibiting the free growth of Fe_3O_4 [27, 28].

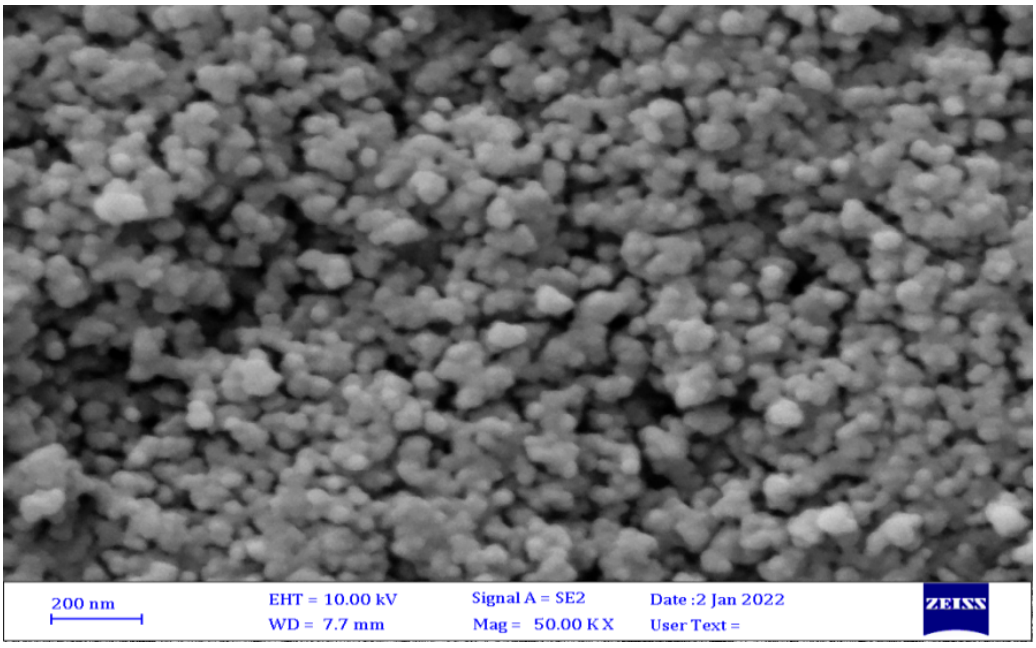

Figure 2. SEM image of Fe_3O_4-Au magnetic nanoparticles.

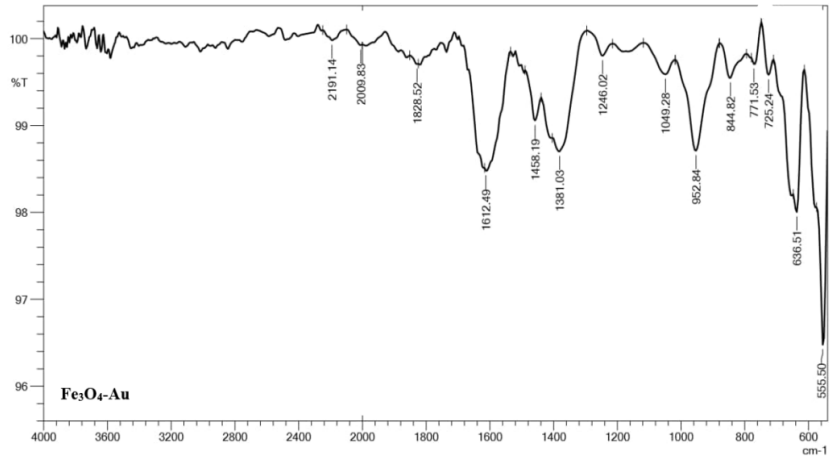

Figure 3. FTIR spectra of Fe_3O_4-Au magnetic nanoparticles.

3.2 Fourier transforms infrared spectra (FTIR)

The structural groups in the wavenumber range of 600 – 4000 cm^{-1} of the Fourier transform infrared (FTIR) spectroscopy are useful indicators of the chemical composition of gases, liquids, powders, and films. The compound's functional groups and chemical bonds are both identified. Fe_3O_4/Au NPs' FTIR spectrum, which has a wide peak in the middle, is depicted in Fig. 3. Fe-O vibrations also have two peaks at 1381.03 and 555.50 cm^{-1}, which are vibrational peaks of Fe_3O_4 NPs [145]. The peaks that appeared at 1381.03 cm^{-1} and 555.50 cm^{-1}, are indicative of stretching, and the various modes of Fe-O confirm the presence of crystalline Fe_3O_4. In addition, the C-H groups stretch at 725.24, 844.84, 1458.19, and 1828.52 cm^{-1}. The FTIR spectrum of Fe_3O_4/Au reveals that it contains all of the peaks from both the Au spectrum and the Fe_3O_4 spectrum. Thus, gold was successfully coated onto the Fe_3O_4 NPs. These variations in absorption peaks show that the Fe_3O_4 surface is coated with Au NPs, demonstrating the success of the fabrication of the Fe_3O_4/Au nanocomposite and the placement of Au there [27].

3.3 Anticancer activity of Fe_3O_4-Au MNPs

Fig. 4 demonstrates that after being incubated with Fe_3O_4-Au at all employed doses, the viability of HT-29 cells was decreased; however, the latter concentration was more effective in this regard. In this study, utilizing the crystal violet dye, which is depicted in Fig. 5 (upper panel), We also looked at how the treatments affected the morphology of HT-29 cells. Cell imaging after Fe_3O_4-Au incubation showed significant morphological alterations in the cells, as well as clumping and blockage of cell communication. With the Fe_3O_4-Au being more potent in this regard. However, in the control group, these changes were not seen. Fe_3O_4-Au had a 50% inhibitory concentration (IC50) of 22.68 gmL^{-1} Fig. 6. By introducing various beneficial alterations over the non-Au nanoparticles, Au enhances the therapeutic efficiency of the medications. By making Au more hydrophilic and slowing down glomerular filtration, Au increases the duration that conjugated therapeutic nanoparticles stay in the bloodstream [29, 30]. Fe_3O_4-Au was dissolved in water at various concentrations (6.25, 12.5, 50, and 100 gmL^{-1}) to increase cell death against HT-29

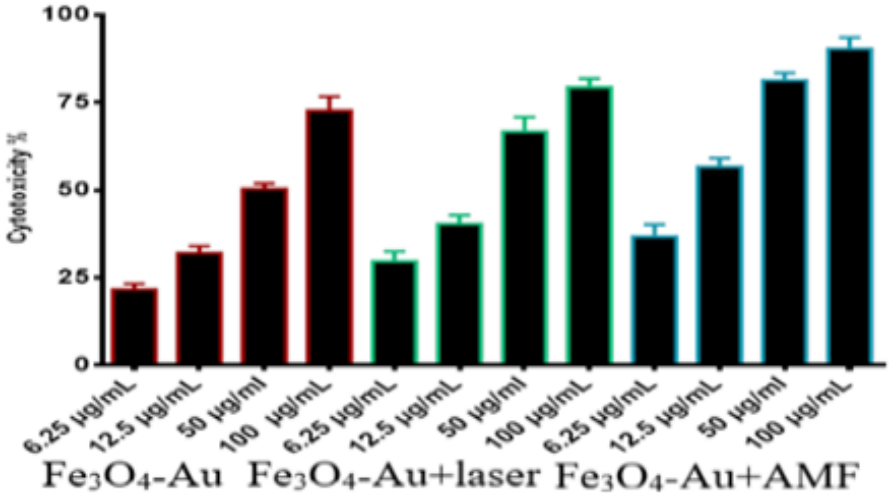

Figure 4. Cytotoxicity of Fe_3O_4-Au nanoparticles in HT-29 Cells.

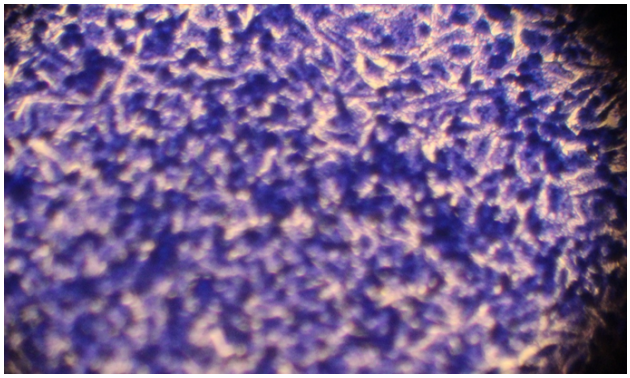

Figure 5. Control untreated HT-29 cells.

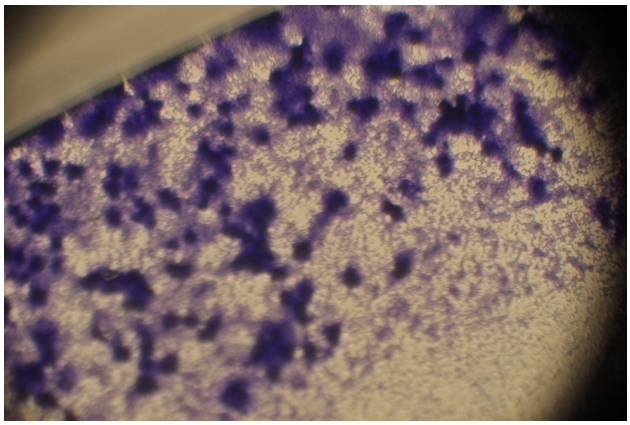

Figure 6. Morphological changes in HT-29 cells after treated with Fe_3O_4-Au NPs.

cells. Fe_3O_4-Au was then subjected to 0.5 w.cm^{-2} of (laser radiation) at an 808 nm wavelength for 20 minutes. After the exposure period, the photothermal action of Fe_3O_4-Au was seen to significantly impede cell development, which resulted in a successful tumor decrease [31]. In this respect, Fe_3O_4-Au was also more effective (see Fig. 6). These results suggest that Fe_3O_4-Au nanoparticles can be taken up by cancerous cells, while laser-treated particles severely damaged cells, laser-untreated particles had a less toxic effect. This is likely due to the photothermal characteristics of the NPs [32]. 17.48 gmL^{-1} is the inhibitory concentration value (IC50) for Fe_3O_4-Au, Fig. 7. If NIR laser or AMF exposure combined, the cells, more HT-29 cells were killed. After being incubated with Fe_3O_4-Au that had been triggered with an NIR laser, the cells' viability was significantly reduced and there was obvious damage to their organelles. The upper and lower panels of Fig. 6 show that Fe_3O_4-Au was also more effective in this regard. The IC50 values for the inhibitory concentrations were Fe_3O_4-Au has a mL^{-1} of 11.63 Fig. 8. The current study's considerable in vitro viability inhibition results show the photothermal impact with an alternating magnetic field's amazing anti-cancer effectiveness [33]. The NPs were given more time and focus, with the latter having the fastest effect, and both samples that were exposed to Fe_3O_4-Au had an increase in temperature as a result. These results show that the Fe_3O_4-Au NPs were suspended in aqueous solution with a high-speed, high-energy conversion efficiency. Previously, this was justified by the hypothesis that after being exposed to 42 °C for 30 minutes, cancer cells may be eliminated. When using temperatures up to 50 °C, this time frame can easily be shortened to 5 minutes. Approximately 36 to 37 °C is the usual body temperature. This approach efficiently heats the cancer cells to 50 °C for 5 minutes by combining the incubation of Fe_3O_4-Au [34]. The long-term toxicity of Fe_3O_4-Au nanoparticles and the ability of HT-29 cells to survive were investigated in the presence and absence of (NIR lasers and AMF) using a clonogenic experiment. These outcomes are consistent with those produced by MTT and crystal violet staining. In contrast to the colonies of the untreated cells, Fig. 6 shows minor toxicity and a decrease in the number of HT-29 cell colonies in the nanoparticle-treated group. AMF and NIR lasers were used to induce, and strong cell-killing abilities were shown in Figs. (7, 8). However, the rapidly decreased clonogenic potential would support the theory that cancer cells that were gradually exposed to Fe_3O_4-Au nanoparticles were killed in a short period of time, which abruptly ended the loss of clonogenic potential. It has been demonstrated in the past that magnetic NPs may limit cell viability by inducing it through processes like apoptosis or necrosis [35].
Figs. 6, 7, and 8 display the findings of this investigation.

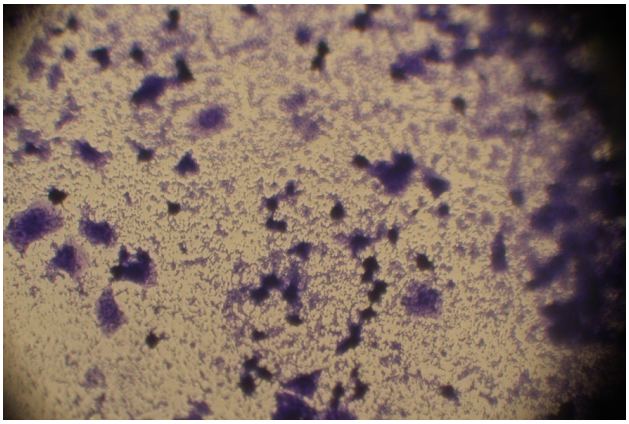

Figure 7. Morphological changes in HT-29 cells after treated with Fe_3O_4-Au NPs + Laser.

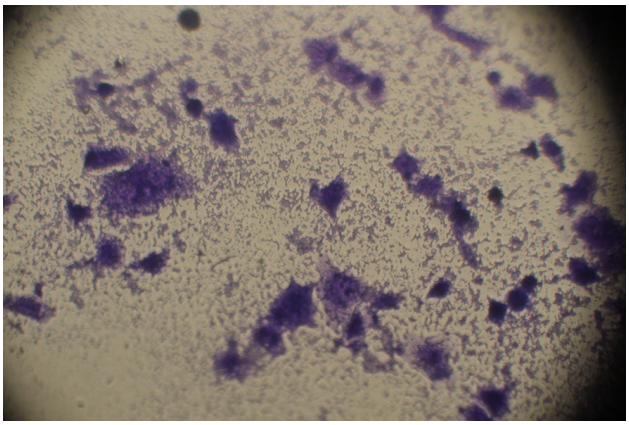

Figure 8. Morphological changes in HT-29 cells after treated with Fe_3O_4-Au NPs + AMF.

The outcomes revealed the generated Fe_3O_4-Au magnetic nanoparticles' capacity to kill colon cancer cells. The effectiveness of Fe_3O_4-Au against cancer cells depends on its concentration, and it is enhanced by the presence of magnetic and laser fields.

4. Conclusion

By using a hydrothermal approach to manufacture the magnetite nanoparticles, Fe_3O_4 with an Au cap, it was possible to see that the agglomeration had been reduced. Fe_3O_4 nanoparticles were coated with Au as a protective coating. Au unregulated the therapeutic efficiency of Fe_3O_4 nanoparticles since it had numerous advantageous differences from non-Au Fe_3O_4 nanoparticles. Au lengthens the period that conjugated nanoparticles circulate in the body by enhancing their hydrophilicity and lowering their rate of glomerular filtration. Results of the current study showed that photothermal effects are highly effective in the treatment of cancer, with in vitro data showing a considerable reduction in cancer cell viability. The spherical Fe_3O_4 NPs were subjected to NIR-induced hyperthermia, which likewise effectively slowed the proliferation of cells. When Fe_3O_4 was covered in Au and subjected to the heating caused by AMF, In HT-29 cells, the morphological alterations were more pronounced. The photothermal effects of magnetic iron oxide can also help cancer therapy methods.

Ethical approval
This manuscript does not report on or involve the use of any animal or human data or tissue. So the ethical approval is not applicable.

Authors Contributions
All the authors have participated sufficiently in the intellectual content, conception and design of this work or the analysis and interpretation of the data (when applicable), as well as the writing of the manuscript.

Availability of data and materials
The datasets generated and analyzed during the current study are available from the corresponding author upon reasonable request.

Conflict of Interests
The author declare that they have no known competing financial interests or personal relationships that could have appeared to influence the work reported in this paper.

References

[1] A. G. Ranjbary, J. Mehrzad, H. Dehghani, A. Abdollahi, and S. Hosseinkhani. "Variation in blood and colorectal Epithelia's Key Trace elements along with expression of mismatch repair proteins from localized and metastatic colorectal cancer patients.". *Biol Trace Elem Res.*, **2**:629, 2020.

[2] G. Mauri, A. Sartore-Bianchi, A. G. Russo, S. Marsoni, A. Bardelli, and S. Siena. "Early-onset colorectal cancer in young individuals.". *Mol Oncol.*, **13**:109–131, 2019.

[3] R. L. Siegel, C. D. Jakubowski, S. A. Fedewa, A. Davis, and N. S. Azad. "Colorectal cancer in the young: Epidemiology, prevention, management. ". *American Society of Clinical Oncology - Educational Book*, **40**:1–14, 2020.

[4] M. Arruebo, N. Vilaboa, B. Sáez-Gutierrez, J. Lambea, A. Tres, M. Valladares, and A. González-Fernández. "Assessment of the evolution of cancer treatment therapies.". *Cancers (Basel)*, **3**:3279–330, 2011.

[5] P. Hassanzadeh, I. Fullwood, S. Sothi, and D. Aldulaimi. "Cancer nanotechnology.". *Gastroenterol Hepatol Bed Bench*, **4**:63–9, 2011.

[6] F. Boateng and W. Ngwa. "Delivery of nanoparticle-based radiosensitizers for radiotherapy applications.". *Int J Mol Sci.*, **21**:273, 2019.

[7] C. Y. Zhao, R. Cheng, Z. Yang, and Z. M. Tian. "Nanotechnology for cancer therapy based on chemotherapy.". *Molecules*, **4**:826, 2018.

[8] A. Ali, H. Zafar, M. Zia, I. Ul Haq, A. R. Phull, J. S. Ali, and A. Hussain. "Synthesis, characterization, applications, and challenges of iron oxide nanoparticles. ". *Nanotechnol Sci Appl.*, **9**:49–67, 2016.

[9] S. Jabir Majid, M. Nayef Uday, K. Abdulkadhim Waleed, and M. Sulaiman Ghassan. "Supermagnetic Fe_3O_4-PEG nanoparticles combined with NIR laser and alternating magnetic field as potent anti-cancer agent against human ovarian cancer cells. ". *Materials Research Express*, **6**:11, 2020.

[10] F. Namvar, H. S. Rahman, R. Mohamad, J. Baharara, M. Mahdavi, E. Amini, M. S. Chartrand, and S. K. Yeap. "Cytotoxic effect of magnetic iron oxide nanoparticles synthesized via seaweed aqueous extract.". *Int J Nanomedicine.*, **9**:2479–88, 2014.

[11] S. Kanagesan, M. Hashim, S. Tamilselvan, N. B. Alitheen, I. Ismail, A. Hajalilou, and K. Ahsanul. "Synthesis, characterization, and cytotoxicity of iron oxide nanoparticles. ". *Advances in Materials Science and Engineering*, **2013**:1–7, 2013.

[12] M. Wu and S. Huang. "Magnetic nanoparticles in cancer diagnosis, drug delivery and treatment. ". *Mol Clin Oncol.*, **7**:738–746, 2017.

[13] A. Manke, L. Wang, and Y. Rojanasakul. "Mechanisms of nanoparticle-induced oxidative stress and toxicity. ". *BioMed Research International*, **2013**, 2013.

[14] Z. Yu, Q. Li, J. Wang, Y. Yu, Y. Wang, Q. Zhou, and P. Li. "Reactive oxygen species-related nanoparticle toxicity in the biomedical field.". *Nanoscale Res Lett.*, **15**:15, 2020.

[15] M. S. Jabir, U. M. Nayef, W. K. Abdulkadhim, Z. J. Taqi, G. M. Sulaiman, U. I. Sahib, A. M. Al-Shammari, et al. "Fe_3O_4 nanoparticles capped with PEG induce apoptosis in breast cancer AMJ13 cells via mitochondrial damage and reduction of NF-κB translocation. ". *Journal of Inorganic and Organometallic Polymers and Materials*, **31**:1241–1259, 2021.

[16] K. Abdulkadhim Waleed and A. Mohammed Mahdi. "Preparation of Fe_3O_4-Au @ Fe_3O_4-Ag composite nanoparticles and cytotoxicity study of kidney parameters in mice.". *Nanomed Res J.*, **7**:227–234, 2022.

[17] A. Waleed, J. Majid, and N. Uday. "A study of kidney parameters in mice induces by super magnetic Fe_3O_4 nanoparticles capped with PEG.". *Research Journal of Biotechnology.*, **14**:89–93, 2019.

[18] Y. W. Huang, M. Cambre, and H. J. Lee. "The toxicity of nanoparticles depends on multiple molecular and physicochemical mechanisms. ". *Int J Mol Sci.*, **18**: 2702, 2017.

[19] H. Lujan and C. M. Sayes. "Cytotoxicological pathways induced af ter nanoparticle exposure: studies of oxidative stress at the 'nano-bio' interface. ". *Toxicol Res (Camb).*, **6**:580–594, 2017.

[20] P. P. Fu, Q. Xia, H. M. Hwang, P. C. Ray, and H. Yu. "Mechanisms of nanotoxicity: generation of reactive oxygen species.". *Journal of Food and Drug Analysis*, **22**:64–75, 2014.

[21] Z. Yu, Q. Li, J. Wang, Y. Yu, Y. Wang, Q. Zhou, and P. Li. "Reactive oxygen species-related nanoparticle toxicity in the biomedical field.". *Nanoscale Research Letters*, **15**:1–4, 2020.

[22] A. G. Al-Ziaydi, A. M. Al-Shammari, M. I. Hamzah, H. S. Kadhim, and M. S. Jabir. "Hexokinase inhibition using D-Mannoheptulose enhances oncolytic newcastle disease virus-mediated killing of breast cancer cells. ". *Cancer Cell International*, **20**:1–10, 2020.

[23] H. N. K. Al-Salman, T. Ali Eman, M. Jabir, M. Sulaiman Ghassan, and A. S. Al-Jadaan Shaker. "2-Benzhydrylsulfinyl N hydroxyacetamide Na extracted from fig as a novel cytotoxic and apoptosis inducer in SKOV 3 and AMJ 13 cell lines via P53 and caspase 8 pathway.". *Eurpean Food Research and Technology.*, **246**:1591–1608, 2020.

[24] S. H. Kareem, A. M. Naji, J. T. Zainab, and S. J. Majid. "Polyvinylpyrrolidone Loaded-MnZnFe 2 O 4 magnetic nanocomposites induce apoptosis in cancer cells through mitochondrial damage and P^{53} pathway. ". *Journal of Inorganic and Organometallic Polymers and Materials*, **30**:5009–5023, 2020.

[25] A. J. Mustafa, T. M. Noori Farah, S. Jabir Majid, S. Albukhaty, A. AlMalki Faizah, and A. Alyamani Amal. "Polyethylene glycol functionalized graphene oxide nanoparticles loaded with Nigella sativa extract: A smart antibacterial therapeutic drug delivery system.". *Molecules*, **26**:3067, 2021.

[26] L. Tonthat, M. Kimura, T. Ogawa, N. Kitamura, Y. Kobayashi, K. Gonda, and S. Yabukami. "Development of gold-coated magnetic nanoparticles as a theranostic agent for magnetic hyperthermia and CT imaging applications.". *AIP Advance.*, **13**:025239, 2023.

[27] H. Danafar, Y. Baghdadchi, M. Barsbay, M. Ghaffarlou, N. Mousazadeh, and A. Mohammadi. "Synthesis of Fe_3O_4-Gold hybrid nanoparticles coated by bovine serum albumin as a contrast agent in MR imaging. ". *Heliyon*, **9**:e13874, 2023.

[28] M. De Luca, D. Marra, A. Acunzo, V. Iannotti, B. Della Ventura, and R. Velotta. "Fe_3O_4@Au core satellite magnetic nanoparticles to enhance colorimetric immunosensor response.". *Optical Sensors* ., **12572**:1257200–1, 2023.

[29] J. Estelrich and M. A. Busquets. "Iron oxide nanoparticles in photothermal therapy. ". *Molecules*, **23**:1567, 2018.

[30] M. Magro, A. Venerando, A. Macone, G. Canettieri, E. Agostinelli, and F. Vianello. "Nanotechnology-based strategies to develop new anticancer therapies. ". *Biomolecules*, **10**:735, 2020.

[31] S. Rajkumar and M. Prabaharan. "Theranostics based on iron oxide and gold nanoparticles for imaging-guided photothermal and photodynamic therapy of cancer.". *Medicinal Chemistry*, **17**:1858–1871, 2017.

[32] E. Kozma, M. Bojtár, and P. Kele. "Bioorthogonally assisted phototherapy: recent advances and

prospects.". *Angew Chem Int Ed Engl.*, **62**: e202303198, 2023.

[33] S. Jahangiri, S. Khoei, S. Khoee, M. Safa, S. Shirvalilou, and V. Pirhajati Mahabadi. "Potential antitumor activity of 13.56 MHz alternating magnetic hyperthermia and chemotherapy on the induction of apoptosis in human colon cancer cell lines HT29 and HCT116 by up-regulation of Bax, cleaved caspase 3&9, and cleaved PARP proteins. ". *Cancer Nanotechnology*, **34**:12, 2021.

[34] Y. Mostafa, K. Shameli, Z. Hedayatnasab, S-Y. Teow, U. N. Ismail, A. A. Che, and R. Rasit Ali. "Green synthesis of Fe_3O_4 nanoparticles for hyperthermia, magnetic resonance imaging and 5-fluorouracil carrier in potential colorectal cancer treatment.". *Research on Chemical Intermediates*, **47**:1789–1808, 2021.

[35] S. Fernandes, T. Fernandez, and S. Metze. "Magnetic nanoparticle-based hyperthermia mediates drug delivery and impairs the tumorigenic capacity of quiescent colorectal cancer stem cells.". *ACS Appl. Mater.*, **13**: 15959–15972, 2021.